IEEE Journal of Selected Topics in Applied Earth Observations and Remote Sensing, Vol. 11, Issue 3, March 2018, pp. 930-938
DOI:10.1109/JSTARS.2018.2799234

Harvest monitoring of Kenyan Tea Plantations with X-band SAR

Boris Snapir, Toby W. Waine, Ronald Corstanje, Sally Redfern, Jacquie De Silva, and Charles Kirui

***Abstract*—Tea is an important cash crop in Kenya, grown in a climatically restricted geographic area where climatic variability is starting to affect yield productivity levels. This paper assesses the feasibility of monitoring tea growth between, but also within fields, using X-band COSMO-SkyMed SAR images (5 images at VV polarisation and 5 images at HH polarisation). We detect the harvested and non-harvested areas for each field, based on the loss of interferometric coherence between two images, with an accuracy of 52% at VV polarisation and 74% at HH polarisation. We then implement a normalisation method to isolate the scattering component related to shoot growth and eliminate the effects of moisture and local incidence angle. After normalisation, we analyse the difference in backscatter between harvested and non-harvested areas. At HH polarisation, our backscatter normalisation reveals a small decrease (~ 0.1 dB) in HH backscatter after harvest. However, this decrease is too small for monitoring shoot growth. The decrease is not clear at VV polarisation. This is attributed to the predominantly horizontal orientation of the harvested leaves.**

***Index Terms*—Tea, SAR, backscatter normalisation, coherence.**

I. Introduction

TEA is a major cash crop for Kenya and is an important economic driver for rural development [1]. Tea (*Camellia Sinensis*) plantations are concentrated in geographically restricted climatic regions and productivity levels are already being affected by increasing climatic variability — reduced and erratic rainfall, higher rate of hail and frost, and rising temperature. In this context, a better understanding of the drivers and limitations to current production is needed to determine the resilience and security of future production. Field estimates of current tea productivity is uncertain, as tea is produced by a mixture of small holders and in larger estates. There is therefore substantial scope for the use of Remote Sensing (RS) to obtain better, more robust estimates of Tea production.

In Kenya, tea is continuously harvested all year round, with two peak seasons, between March and June and between October and December. Pluckers progressively harvest a given field over several days depending on the amount of tea to harvest and the allocated number of pluckers. Harvesting consists in cutting, by hand or machine, only the tender young shoots at the top of the canopy, with each shoot formed by the apical bud and two to five leaves. Once a field is harvested, it takes 2-3 weeks for new shoots to grow and be ready for harvest again. Monitoring shoot growth at regional scale with RS could (i) improve our understanding of tea yield against climatic conditions and (ii) support decisions in the tea estates' management system for more optimal productivity levels. For example, RS could help decide when/where to harvest or identify under-performing patches of tea in need of further ground assessment. Eventually, RS data reflecting the current state of tea could be integrated to a shoot growth model like Cuppa-tea for improved yield forecast [2], [3].

Previous studies have investigated the use of multispectral RS in North East India to map tea affected by diseases [4], to assess correlation between the Normalised Difference Vegetation Index (NDVI) and tea quality [5], [6], and to monitor the replantation stages of deceased tea [7]. L-band Synthetic Aperture Radar (SAR) was also tested to estimate tea biomass [8], but there has not yet been studies investigating the use of RS for monitoring shoot growth. Considering the climatic conditions of the tea growing area, optical instruments have reduced imaging opportunities. SAR, with its all-weather imaging capability, is a better suited candidate for operational tea monitoring.

Among other parameters (incidence angle, water content, surface roughness), the SAR measurements are sensitive to the structure of the crops; especially for X-band (2.5-3.75 cm) and C-band (3.75-7.5 cm) SARs which have a wavelength similar to the scale of the structural parts of the canopy [9]. The sensitivity of the SAR measurements also depends on the polarisation. For example, vertically oriented crops typically interact more with the vertical polarisation than the horizontal polarisation [10], [11]. The monitoring capability of SAR has been demonstrated particularly for crops which have morphological changes in parallel of their phenological development, as for e.g. for rice [9], [11]–[13], and for cereal crops [14]–[17].

In this study, our hypothesis is that, in between two harvests, shoot growth produces changes at the surface of the tea canopy which could be detected by X-band SAR as a change in surface texture/roughness. X-band is expected to be better suited for detecting the fine surface changes associated with shoot growth than longer wavelengths, which typically have backscattering contributions from the deeper canopy and the underlying soil. We tested this hypothesis with a time series of 10 repeat pass images from the COSMO-Skymed constellation taken over a

(Corresponding author: Ronald Corstanje.)

B. Snapir, T. W. Waine and R. Corstanje are with The School of Water, Energy and Environment, Cranfield University, Cranfield, Bedfordshire, MK43 0AL, UK. (email: b.j.snapir@cranfield.ac.uk; t.w.waine@cranfield.ac.uk; ron-corstanje@cranfield.ac.uk).

S. Redfern and J. De Silva are with Unilever R&D UK Ltd, Colworth Science Park, Sharnbrook, Bedfordshire, MK44 1LQ, UK. (email: Sally.Redfern@unilever.com; Jacquie.De-Silva@unilever.com).

C. Kirui is with R&D Unilever Tea Kenya Ltd, Off Nakuru-Kericho Highway, P.O.Box 20-20200, Kericho, Kenya. (email: Charles.Kirui@unilever.com).

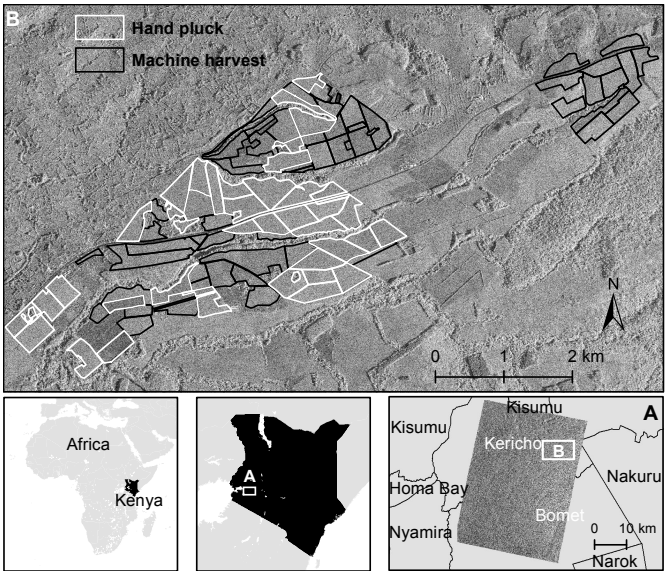

Fig. 1. kapkorech estate with hand pluck (black) and machine harvested (white) fields, and COSMO-SkyMed image from 23 August 2016.

tea estate near Kericho (Kenya). Our results show that the backscatter for the harvested portion of a field is smaller than that for the non-harvested portion, only at HH polarisation (not at VV polarisation), but that this difference is too small for shoot monitoring.

II. Study Area and Materials

A. Study Area

The study area corresponds to the Kapkorech tea estate located near Kericho in the central highlands of Kenya (Africa). The region has a tropical climate and is prone to cloud cover making SAR acquisitions more feasible than optical imagery. The estate is composed of 91 tea fields, among which only 81 were active at the time of the study. The rest of the fields were recovering from previous pruning. The average size of the fields is 10.3 ha. Fig. 1 shows the outline of the fields with in black and white, the fields which are machine harvested (48 fields) and hand pluck (33 fields) respectively. Hand plucking allows selecting individual tea shoots and is labor intensive (Fig. 2b). Machine harvesting removes all the leaves and twigs below a certain canopy depth (Fig. 2c), it is usually associated with lower quality tea.

B. SAR data

Table I lists the characteristics of the 10 COSMO-SkyMed images acquired in Stripmap HIMAGE mode from repeat passes over the study area from the 6^{th} July 2016 to the 8^{th} September 2016. The first 5 images and the last 5 images were acquired in VV polarisation and HH polarisation, respectively. A large incidence angle (50 deg) was selected to minimize canopy penetration as we are interested in measuring changes at the canopy surface. Descending pass (6 pm) was selected to avoid the effect of morning dew, and so that a given image can reflect the harvest activity which took place during the day.

(a)

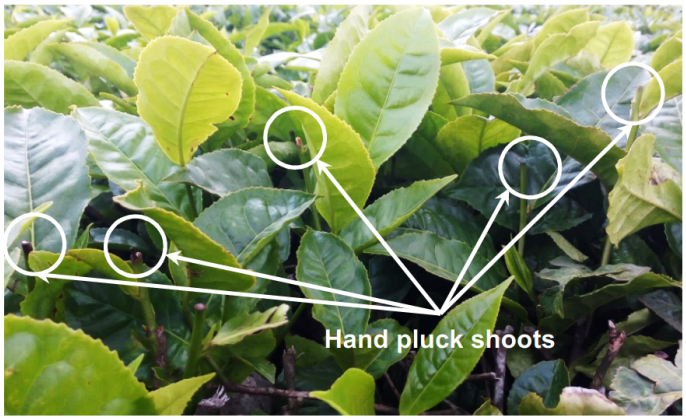

(b)

(c)

Fig. 2. Photos of tea canopy (a) before harvesting, (b) after hand plucking, and (c) after machine harvesting. Hand plucking targets individual young shoots, while machine harvesting removes any leaves/twigs above a certain canopy depth.

TABLE I
(A) TECHNICAL CHARACTERISTICS OF COSMO-SKYMED AND (B) LIST OF THE AVAILABLE IMAGES.

Imaging mode	Stripmap HIMAGE
Processing level	Level 1A
Resolution	2.8 m
Swath width	40 km
Wave length	X-band
Near field incidence	49.6 deg
Far field incidence	50.6 deg
Pass	Descending
Local time	17:56

(A)

Image	Date	Polarisation
1	2016/07/06	VV
2	2016/07/22	VV
3	2016/07/30	VV
4	2016/08/03	VV
5	2016/08/07	VV
6	2016/08/15	HH
7	2016/08/23	HH
8	2016/08/31	HH
9	2016/09/04	HH
10	2016/09/08	HH

(B)

C. Ground observations

Ground observations were collected on the day of each SAR acquisition. Data include photos of each fields harvested on that day and a field sheet. Six photos are taken for each field — 4 photos in the 4 cardinal directions, 1 photo with a overall view of the field, and 1 photo with a close up view of the tea canopy. The field sheet includes a map of the tea estate to report (i) the locations where the photos were taken, (ii) which fractions of fields were harvested on that day, (iii) the harvest method and the typical number of harvested leaves, and (iv) weather observations. Rainfall measurements were available from an automatic rain gauge on site, and monthly harvest reports were provided by the estate, indicating which fields were harvested on each day. Fig. 3 shows a time-line summarising all the available data. The harvest gap between 12 and 24 July corresponds to an unplanned suspension of harvest which limited the analysis of the second SAR image. The chart also shows that individual fields are often harvested over 4-5 days.

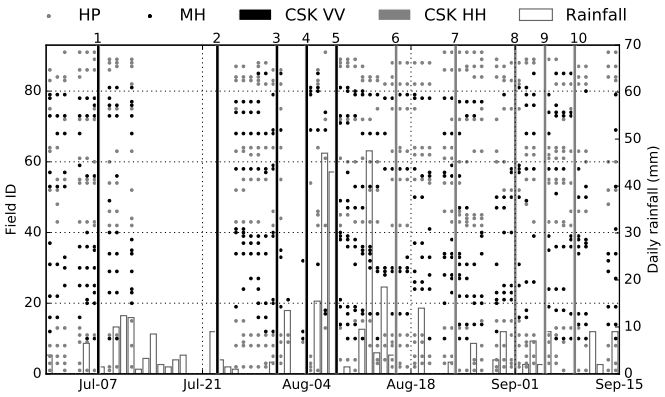

Fig. 3. Time-line of all available data. The gap between 12 and 24 July corresponds to a suspension of harvest. The harvested fields (from the harvest report) are marked with gray and black dots for hand pluck (HP) and machine harvest (MH) respectively. The black and gray narrow bars correspond the 10 COSMO-SkyMed (CSK) acquisitions at VV and HH polarisation respectively. Finally the white bars are the rainfall measurements from the rain gauge.

III. METHODOLOGY

A. Overview

As opposed to crops harvested once or twice a year, tea is continuously harvested making it difficult to identify pre-harvest and post-harvest dates for which the backscatter can be analysed. Instead, our approach takes advantage of the fact that between two acquisition dates, some fields are only partially harvested. The idea is to compare the backscatter of the harvested portion of a field with the backscatter of the non-harvested portion. In practice, the method is composed of two main processing chains (Fig. 4). All the images are first co-registered to the first image (6 July 2016) of the time series. Then, we detect the harvested portion of each field, between 2 image dates, using the loss of interferometric coherence (Fig. 4(a)). This is repeated for each pair of consecutive images with identical polarisation (4 VV pairs and 4 HH pairs). With the second processing chain, we derive a backscatter coefficient with ad hoc radiometric normalisation to limit the effect of variations in moisture and local incidence angle (Fig. 4(b)). After normalisation, we computed the backscatter of the harvested and non-harvested portions of each field, for the second image of each pair. For a given image pair, the area detected as non-harvested may have been harvested before the first image or after the second image, while the area detected as harvested has been harvested some time between the first and the second image (Fig. 5a). The maximum backscatter difference between harvested and non-harvested areas can be expected when the harvest took place soon before the second image (Fig. 5b), as the shoots would not have grown significantly on the day where the backscatter is computed (image $i+1$).

B. Detection of harvested areas

Using the Sentinel Application Platform (SNAP), we computed the coherence between consecutive images with identical polarisation and applied terrain correction. We then processed the terrain-corrected coherence with scripts written in Python. For a given coherence image, we extracted the coherence of a field using its field geometry (Fig. 6a), applied a 31x31-pixel averaging window (Fig. 6b), and extracted the harvested and non-harvested masks using a simple threshold (Fig. 6d). Although the coherence over tea fields is relatively low (0.1-0.3) — characteristic of coherence over vegetation — when tea pluckers walk across a field, they disturb the canopy and this can be captured by a decrease in coherence. A threshold value of 0.22 was selected after applying Otsu's method [18] to the fields with known harvested area. Note that some discrepancies remain between detected harvested area and the field sheets (Fig. 6d, 6e) because the latter are only indicative of the actual harvested area. After thresholding, we rejected the detected

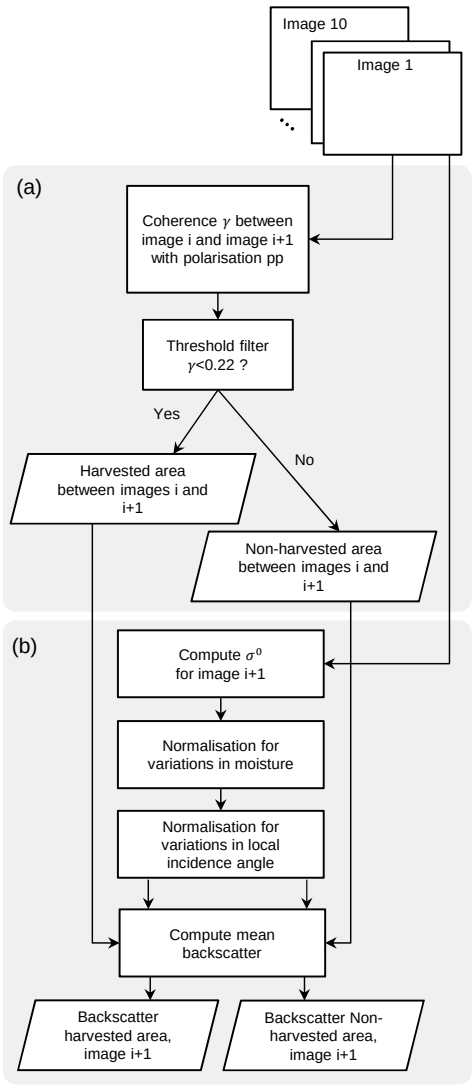

Fig. 4. The methodology is implemented in two main processing chain. First (a), the harvested area is detected for each field using the loss of coherence between successive images. Then (b), for the second image of each pair, the normalised backscatter values for the harvested and non-harvested portions of each field are compared.

harvested areas which were smaller than 0.1 ha, to limit false positives due to noisy coherence. This approach significantly complements the field observations. The latter shows the portions of fields which have been harvested on the day of a SAR acquisition, but it does not say anything about the rest of the fields which may or may not have been harvested a few days before. With the loss of coherence, a portion detected as harvested suggests that it has been harvested at some point between the first and the second date of the image pair. Similarly, a portion detected as non-harvested has not been harvested for at least the time duration between the first and the second image of the pair.

C. Backscatter normalisation

The hilly topography of the region complicates intra-field comparison of backscatter because the scattering depends on the local incidence angle. This dependency was confirmed by

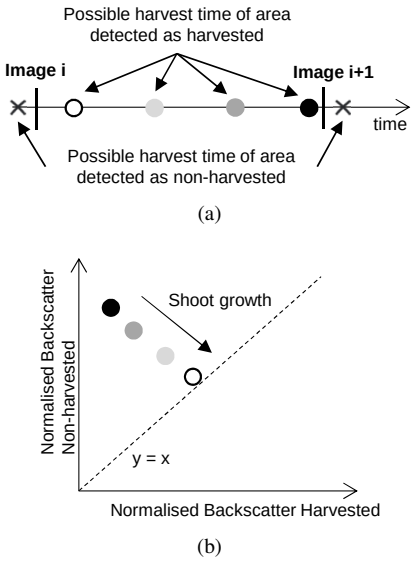

Fig. 5. Interpretation of the expected results. (a) For a given field, the area detected as harvested was harvested between image i and image $i+1$, while the non-harvested area was harvested before image i and/or after image $i+1$. In a scatter plot with harvested and non-harvested backscatter (b), the largest backscatter difference is expected when harvest occurs close to the date of image $i+1$ (black dot). Here we assume that the harvested backscatter is smaller than the non-harvested backscatter.

cross-checking spatial variations in backscatter with the available ground photos showing an overview of the tea fields and their topography. Various radiometric terrain corrections have been developed to remove bakscatter variations due to changes in local incidence angle (sine/cosine correction, backscatter simulation, first/second order regression, fequency/histogram matching) [19], [20]. These techniques require an accurate Digital Terrain Model (DTM) of the imaged area to derive the local incidence angle. In absence of a DTM with sufficiently high resolution to capture the within-field topography, we applied a relative backscatter normalisation for each field (Fig. 7). First, we removed the overall temporal changes across the different image dates that were attributed to variations in moisture (Fig. 7b). Moisture measurements are not available, but the rainfall measurements on Fig. 3 suggest that strong variations in moisture can be expected across the image dates. Assuming that moisture is uniform over a given field, we attenuated the effect of moisture by subtracting the field-average backscatter to each pixel. We then attenuated the effect of within-field variations in local incidence angle (Fig. 7c). As the local incidence angle is the same across the time series of images (repeat pass images), we isolated its backscatter effect by computing the time average of each pixel. We then subtracted this time average from each image. More precisely, to limit temporal variations due to speckle, the time average was computed for a spatial window of 31x31 pixel centred on the pixel being normalised. Note that this incidence normalisation will also attenuate spatial heterogeneity (constant over time) in moisture not removed when subtracting the field average, i.e. moisture heterogeneity will be treated as variation in local incidence angle. The remaining spatial and temporal variations in backscatter are expected to be solely related to the state of the tea shoots.

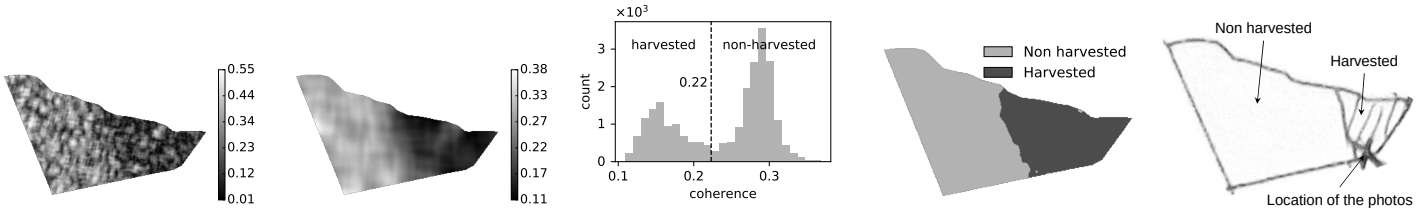

(a) (b) (c) (d) (e)

Fig. 6. Processing steps to detect harvested and non-harvested areas for a given field, with (a) the raw coherence between images i and $i+1$ extracted for a given field, (b) the coherence after spatial averaging, (c) the thresholding of the bi-modal histogram of the coherence, (d) the mask of harvested and non-harvested areas, and (e) the corresponding field sheet indicative of the harvested area.

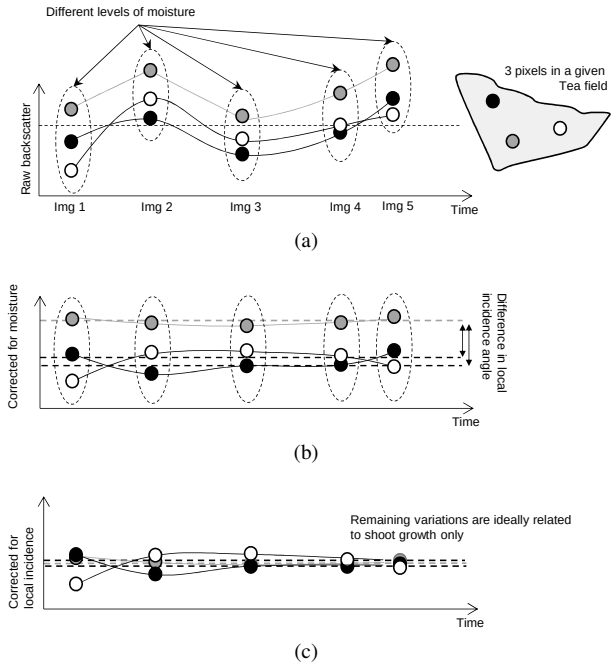

(a)

(b)

(c)

Fig. 7. Relative normalisation of the backscatter coefficient. Some of the variations in the raw backscatter coefficient are due to variations in moisture and local incidence angle (a). The effect of moisture is removed by subtracting the field average to each pixel for each image (b). The effect of local incidence angle is then removed by subtracting to a pixel, the temporal average of a 31x31 pixel window centred on that pixel (c).

TABLE II
ACCURACY ASSESSMENT OF THE DETECTION OF HARVESTED FIELD BASED ON COHERENCE LOSS (A) FOR THE VV-POLARISED IMAGE PAIRS AND FOR THE (B) HH-POLARISED IMAGE PAIRS. *Baseline* AND *rain* ARE THE NUMBER OF DAYS AND THE RAIN BETWEEN THE TWO IMAGES OF EACH PAIR. IMAGE PAIR 4-5 WAS EXCLUDED FROM THE TOTAL, HEAVY RAINFALL PRIOR TO IMAGE 5 CAUSED ALL FIELDS TO BE DETECTED AS HARVESTED.

Polarisation	VV				
Image pair	1-2	2-3	3-4	4-5	
Baseline (days)	16	8	4	4	**Total**
Rain (mm)	67	5	14	106	
True pos.	35	35	15	25	85
True neg.	6	18	23	0	67
Total (%)	45	58	42	27	52
False pos.	50	38	52	66	140
False neg.	0	0	1	0	1
Total (%)	55	42	58	73	48

(A)

Polarisation	HH				
Image pair	6-7	7-8	8-9	9-10	
Baseline (days)	8	8	4	4	**Total**
Rain (mm)	16	18	11	0	
True pos.	39	46	34	30	149
True neg.	15	22	43	40	120
Total (%)	59	75	85	77	74
False pos.	37	23	14	19	93
False neg.	0	0	0	2	2
Total (%)	41	25	15	23	26

(B)

IV. RESULTS

A. Detection of harvested areas - Accuracy assessment

Assessing the accuracy of the coherence method to detect harvested areas would require knowing the areas harvested between each SAR images. In practice, ground observations are only available for the SAR dates, and the harvest report solely indicates which fields were harvested on each day without spatial information on the harvested areas. Our accuracy assessment consisted in cross-checking which fields were or were not harvested between two image dates against the harvest report. In Table II, true positives and true negatives are fields rightly detected as harvested and non-harvested respectively, and false positives and false negatives are fields wrongly detected as harvested and non-harvested respectively. Overall, the detection method is prone to false positives, this is because perturbations, like wind or rain, can disturb the tea canopy and lead to coherence below the detection threshold. For example, for image pair 4-5, all the fields were detected as fully harvested. The rain measurements on Fig. 3 suggest that heavy rainfalls (106 mm) between images 4 and 5 must have caused the coherence below 0.22. Overall, the detection accuracy is 52% at VV polarisation, and 74% at HH polarisation. This difference can be explained by the adverse conditions during the VV acquisitions — rainfall for image pairs 1-2 and 4-5, suspension of harvest for image pair 2-3. Wind data would also be needed to further explain the difference. Although incomplete, this accuracy assessment shows that reliable harvest detection requires clear weather condition and short temporal baseline.

Prior to comparing the backscatter for harvested and non-harvested areas, we visually inspected the detected harvested area for the true positives and selected only those showing a

clear delineation of harvested and non-harvested areas. Indeed, the shape of the detected harvested area may be inaccurate because of noisy coherence (random areas with low coherence). Out of the 234 true positives (excluding image pair 4-5), 99 were selected for the backscatter analysis, including 27 which were validated against the ground observations. These 99 cases correspond to 40 different fields (out of 81 active fields), with some of them being selected multiple times (maximum 6 times) and others only once. This selection includes 24 hand-pluck and 16 machine-harvested fields, thus we expect it to be representative of the various field conditions of the estate. Note that this selection excludes cases where fields are fully harvested or fully not-harvested. In the following sections, we compare the mean backscatter for the harvested and non-harvested portions of these 99 cases.

B. Backscatter normalisation

To highlight the necessity of normalising the backscatter coefficient, Fig. 8 shows the comparison between harvested and non-harvested backscatter without normalisation. In this case, the incidence angle used to derive the bakscatter coefficient is computed using an ellipsoid Earth model. For both VV and HH polarisations, there is no clear separation between harvested and non-harvested backscatter – the partitioning to the left and right of the $y = x$ line is 47%-53% for VV and 51%-49% for HH. In comparison, after normalisation (Fig. 9), at HH polarisation, the non-harvested backscatter is larger than the harvested backscatter for all the points validated by the ground observations, and for the majority of the other points (75%-25% partition). The separation is less clear at VV polarisation (55%-45%) — two of the validated points go against the trend observed at HH polarisation.

C. Sensitivity to shoot growth

While the scatter plots suggest that the backscatter decreases with harvest, the difference cannot be used for shoot growth monitoring as it is too small ($\sim$ 0.1 dB) compared to the typical radiometric accuracy ($\sim$ 1 dB) of current spaceborne SAR. The decrease in backscatter tends to be more significant for machine harvested fields (circle markers) than for hand pluck fields (triangle markers). This is consistent with the fact that machine harvesting systematically removes the top few centimeters of tea canopy, while hand plucking is more selective (see photos Fig.2). The overall horizontal orientation of unfolding young leaves on the harvested tea shoots could explain the better sensitivity at HH polarisation. The young leaves are also comparable in size to the radar wavelength at X-band (3.1 cm). This interaction with young leaves may result in surface scattering characterised by little depolarisation effect, hence a stronger HH backscatter before harvest of the shoots. After harvest, the surface scattering may be replaced by more volume scattering characterised by stronger depolarisation effect in the old canopy composed of randomly oriented leaves. In comparison, at VV polarisation, there may be some interactions with the vertically oriented apical buds of young shoots, but not as significant as the interaction with the young leaves at HH polarisation. The time separation between harvest and image date was derived from the tea estate's harvest report, but no correlations were found with the distance of the points to the $y = x$ line, as anticipated in Fig. 5. This is also visible on Fig. 9, the validated points correspond to freshly harvested fields (harvested on the day of the second image of each image pair), but they are not the furthest away from the $y = x$ line. In summary, the distribution of points on the scatter plots (Fig. 9) is definitely related to harvest, but the sensitivity is too small for monitoring shoot growth.

V. Discussion

A. Detection of harvested area

The detection of harvested areas using the coherence was prone to false detections because rain can disrupt the tea canopy and lead to loss of coherence. Using longer wavelength like C- or L-band could provide more robust coherence measurements. At longer wavelength, the penetration depth of SAR measurements increases, thus elements below the surface canopy, like small branches, contribute to the scattering. These small branches will still be disrupted by pluckers, but they may not be affected by rain as much as the top canopy, hence the improvement in coherence measurement. This could not be tested with Sentinel-1 images as the available repeat-pass images over the study area at the time of the study were separated by 24 days resulting in significant temporal decorrelation.

B. Monitoring shoot growth

Although optical remote sensing may not be suitable for monitoring shoot growth due to frequent cloud cover, a cloud-free optical image from Sentinel-2 (not shown in this paper) acquired during our experiment suggests that shoot growth translates into an increase in Normalised Difference Vegetation Index (NDVI) (increase of 0.1 between harvested and non-harvested areas). Future research could use full polarimetric imagery from TerraSAR-X (X-band), Radarsat-2 (C-band), or ALOS-2 (L-band), to assess the sensitivity of backscatter ratios such as the Radar Vegetation Index (RVI). The RVI reflects the amount of depolarisation from volume scattering and was shown to behave closely to the NDVI when monitoring rice and soybean at L-band [21]. Polarimetric decomposition, like the H-A-alpha decomposition, could also be used to further understand the scattering mechanisms of tea plants and how these mechanisms may change with shoot growth [10].

C. Backscatter normalisation

Our two-step normalisation procedure enhanced small differences in backscatter between harvested and non-harvested areas by effectively removing temporal variations in moisture and spatial variations in local incidence angle. More generally, this method could also be adapted to detect intra-field variations especially for crops with strong morphological changes like rice [22].

An experiment including measurements of vegetation water content would be needed to confirm that the field-average

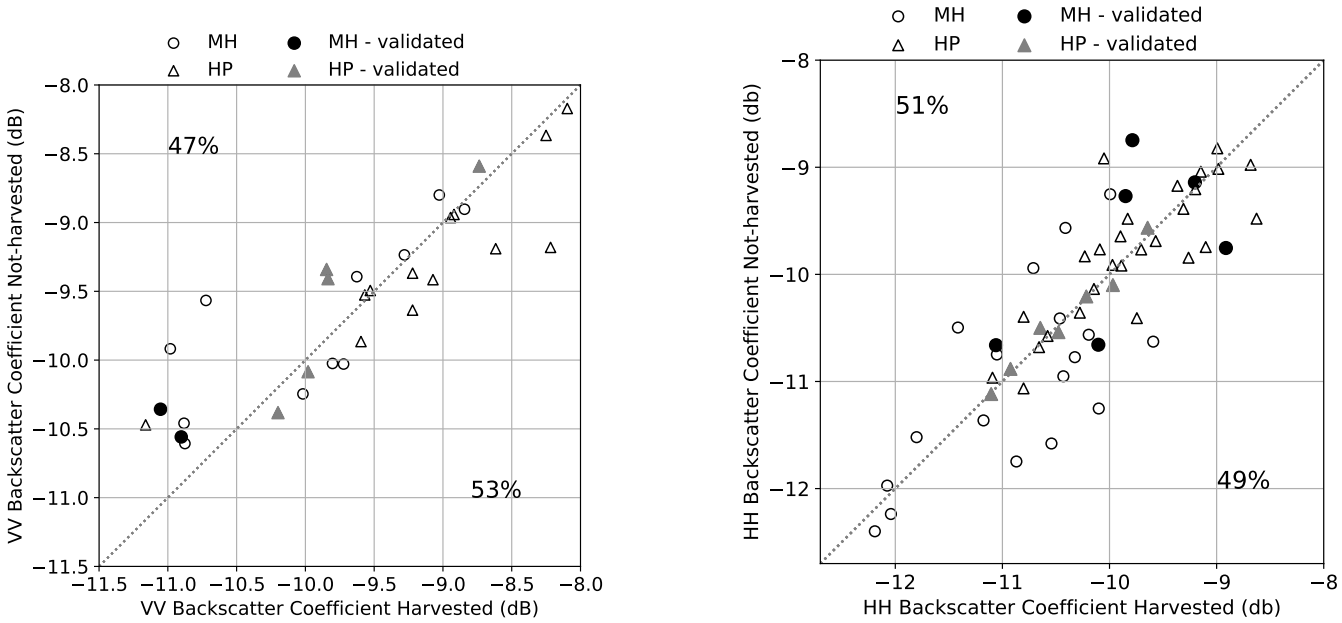

(a) (b)

Fig. 8. Mean backscatter coefficient of the non-harvested portion of a field against that of the harvested portion for (a) the VV polarised images and (b) the HH polarised images. The circle markers and triangle markers are for machine-harvested (MH) and hand-pluck (HP) fields respectively. The black dots and gray triangles highlight the MH and HP fields respectively, for which the harvested and non-harvested area was confirmed by the ground observations.

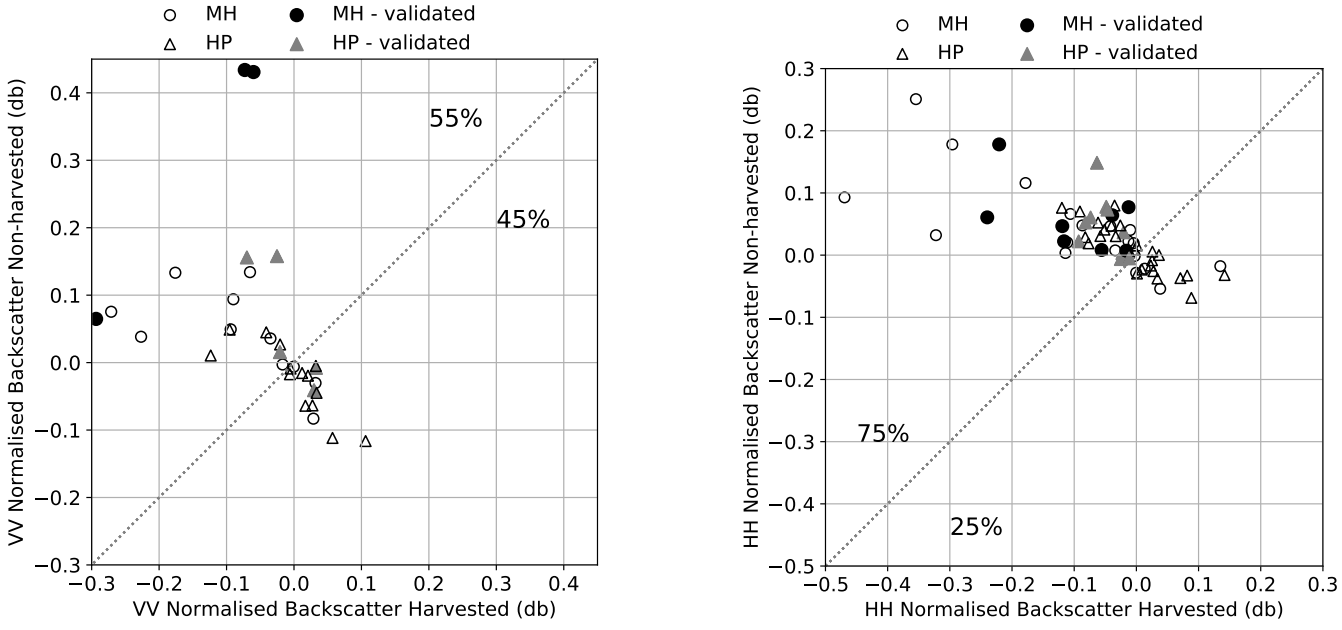

(a) (b)

Fig. 9. Mean normalised backscatter of the non-harvested portion of a field against that of the harvested portion for (a) the VV polarised images and (b) the HH polarised images. The circle markers and triangle markers are for machine-harvested (MH) and hand-pluck (HP) fields respectively. The black dots and gray triangles highlight the MH and HP fields respectively, for which the harvested and non-harvested area was confirmed by the ground observations.

backscatter is indeed related to vegetation moisture. Eventually, abnormally-low basckatter value could be related to water stress. Several studies have demonstrated the capability of SAR to retrieve soil moisture using change detection, with change in vegetation cover complicating the retrieval [23], [24]. A similar approach could be implemented to retrieve tea canopy moisture. Unlike crops with strong morphological changes, tea is managed so that the canopy surface remains accessible by pluckers, therefore canopy moisture is anticipated to be the dominant changing parameter affecting the radar backscatter, making change detection unambiguous.

VI. Conclusion

We investigated the capability of X-band SAR to monitor tea shoot growth using a time series of COSMO-SkyMed images for regional monitoring. Our approach attempted to disentangle the multiple scattering contributions (moisture, local incidence angle, physical geometry of target) affecting the backscatter measurements to isolate the scattering component related to shoot development. We took advantage of the fact that tea is continuously harvested with some fields being only partially harvested on a given day, so that the backscatter of the harvested portion can be compared to that of the non-harvested portion. We used the loss of coherence between two successive images to separate the harvested and non-harvested portions of each field with an accuracy of 52% at VV polarisation and 74% at HH polarisation. This method is prone to false positive as there can be a loss of coherence because of wind/rain. However, results show that our backscatter normalisation reveals differences in backscatter between harvested and non-harvested areas, not visible in the raw backscatter coefficient. At HH polarisation, there was a decrease in backscatter ($\sim$0.1 dB) after harvest for 73% of the fields, too small to be used for shoot monitoring. At VV polarisation, results were not conclusive because of the limited number of fields with reliable detection of harvested area.

Future work on tea monitoring in cloud-prone tropical areas like Kenya should consider the use of fully polarimetric imagery to highlight any changes in scattering mechanisms (e.g. RVI, $\sigma^0_{VH}/\sigma^0_{VV}$ ratio, H-A-alpha decomposition).

Acknowledgment

The authors would like to thank Unilever for sponsoring this research, and Telespazio for providing the COSMO-SkyMed imagery.

References

[1] A. Elbehri, B. Cheserek, A. Azapagic, D. Raes, M. Mwale, J. Nyengena, P. Kiprono, C. Ambasa, "KENYA'S TEA SECTOR UNDER CLIMATE CHANGE An impact assessment and formulation of a climate-smart strategy," Food and Agriculture Organisation of the United Nations, Rome, Italy, Tech. Rep., 2015.

[2] R. Matthews and W. Stephens, "Cuppa-tea: A simulation model describing seasonal yield variation and potential production of tea. 2. biomass production and water use," *Experimental Agriculture*, vol. 34, no. 04, pp. 369–389, 1998.

[3] ——, "Cuppa-tea: A simulation model describing seasonal yield variation and potential production of tea. 1. shoot development and extension," *Experimental Agriculture*, vol. 34, no. 04, pp. 345–367, 1998.

[4] R. Dutta, A. Stein, and N. Patel, "Delineation of diseased tea patches using mxl and texture based classification," *The International Archives of the Photogrammetry, Remote Sensing and Spatial Information Sciences*, vol. 37, no. B4, pp. 1693–1700, 2008.

[5] R. Dutta, "Monitoring green leaf tea quality parameters of different TV clones grown in northeast India using satellite data," *Food Chemistry*, vol. 139, no. 1, pp. 689–694, 2013.

[6] R. Dutta, A. Stein, and R. Bhagat, "Integrating satellite images and spectroscopy to measuring green and black tea quality," *Food chemistry*, vol. 127, no. 2, pp. 866–874, 2011.

[7] A. Singh, R. Dutta, A. Stein, and R. M. Bhagat, "A wavelet-based approach for monitoring plantation crops (tea: *Camellia sinensis*) in North East India," *International Journal of Remote Sensing*, vol. 33, no. 16, pp. 4982–5008, Aug. 2012. [Online]. Available: http://www.tandfonline.com/doi/abs/10.1080/01431161.2012.657364

[8] A. Banerjee, "Tea Bush Biomass Assessment Through Polarimetric Decomposition and Semi-empirical Modelling," Ph.D. dissertation, University of Twente, 2012. [Online]. Available: https://www.iirs.gov.in/iirs/sites/default/files/StudentThesis/Banerjee_Abhishek_28155_thesis.pdf

[9] O. Yuzugullu, S. Marelli, E. Erten, B. Sudret, and I. Hajnsek, "Determining Rice Growth Stage with X-Band SAR: A Metamodel Based Inversion," *Remote Sensing*, vol. 9, no. 5, p. 460, 2017.

[10] H. McNairn and B. Brisco, "The application of C-band polarimetric SAR for agriculture: a review," *Canadian Journal of Remote Sensing*, vol. 30, no. 3, pp. 525–542, Jan. 2004. [Online]. Available: http://www.tandfonline.com/doi/abs/10.5589/m03-069

[11] E. Erten, C. Rossi, and O. Yüzügüllü, "Polarization impact in TanDEM-X data over vertical-oriented vegetation: The paddy-rice case study," *IEEE Geoscience and Remote Sensing Letters*, vol. 12, no. 7, pp. 1501–1505, 2015.

[12] F. Vicente-Guijalba, T. Martinez-Marin, and J. M. Lopez-Sanchez, "Crop phenology estimation using a multitemporal model and a Kalman filtering strategy," *IEEE Geoscience and Remote Sensing Letters*, vol. 11, no. 6, pp. 1081–1085, 2014.

[13] A. Nelson, T. Setiyono, A. Rala, E. Quicho, J. Raviz, P. Abonete, A. Maunahan, C. Garcia, H. Bhatti, L. Villano, P. Thongbai, F. Holecz, M. Barbieri, F. Collivignarelli, L. Gatti, E. Quilang, M. Mabalay, P. Mabalot, M. Barroga, A. Bacong, N. Detoito, G. Berja, F. Varquez, E. Wahyunto, D. Kuntjoro, S. Murdiyati, S. Pazhanivelan, P. Kannan, P. Mary, E. Subramanian, P. Rakwatin, A. Intrman, T. Setapayak, S. Lertna, V. Minh, V. Tuan, T. Duong, N. Quyen, D. Van Kham, S. Hin, T. Veasna, M. Yadav, C. Chin, and N. Ninh, "Towards an Operational SAR-Based Rice Monitoring System in Asia: Examples from 13 Demonstration Sites across Asia in the RIICE Project," *Remote Sensing*, vol. 6, no. 11, pp. 10 773–10 812, nov 2014. [Online]. Available: http://www.mdpi.com/2072-4292/6/11/10773/

[14] Y. Li and G. Lampropoulos, "Utilizing both Radarsat-2 And TerraSAR-X polarimetrie data for crop growth stages estimation," in *Digital Signal Processing (DSP), 2017 22nd International Conference on*. IEEE, 2017, pp. 1–5.

[15] A. Sinha, W. Tan, Y. Li, H. McNairn, X. Jiao, and M. Hosseini, "Applying a particle filtering technique for canola crop growth stage estimation in Canada," in *Remote Sensing for Agriculture, Ecosystems, and Hydrology XIX*, C. M. Neale and A. Maltese, Eds. International Society for Optics and Photonics, 2017, p. 55.

[16] F. Canisius, J. Shang, J. Liu, X. Huang, B. Ma, X. Jiao, X. Geng, J. M. Kovacs, and D. Walters, "Tracking crop phenological development using multi-temporal polarimetric radarsat-2 data," *Remote Sensing of Environment*, 2017.

[17] F. Vicente-Guijalba, T. Martinez-Marin, and J. M. Lopez-Sanchez, "Dynamical approach for real-time monitoring of agricultural crops," *IEEE Transactions on Geoscience and Remote Sensing*, vol. 53, no. 6, pp. 3278–3293, 2015.

[18] N. Otsu, "A threshold selection method from gray-level histograms," *IEEE transactions on systems, man, and cybernetics*, vol. 9, no. 1, pp. 62–66, 1979.

[19] I. E. Mladenova, T. J. Jackson, R. Bindlish, and S. Hensley, "Incidence Angle Normalization of Radar Backscatter Data," *IEEE Transactions on Geoscience and Remote Sensing*, vol. 51, no. 3, pp. 1791–1804, mar 2013. [Online]. Available: http://ieeexplore.ieee.org/document/6264094/

[20] D. Small, "Flattening Gamma: Radiometric Terrain Correction for SAR Imagery," *IEEE Transactions on Geoscience and Remote Sensing*, vol. 49, no. 8, pp. 3081–3093, aug 2011.

[21] K. Yihyun, T. Jackson, R. Bindlish, L. Hoonyol, and H. Sukyoung, "Radar Vegetation Index for Estimating the Vegetation Water Content of Rice and Soybean," *IEEE Geoscience and Remote Sensing*

Letters, vol. 9, no. 4, pp. 564–568, jul 2012. [Online]. Available: http://ieeexplore.ieee.org/document/6112792/

[22] O. Yuzugullu, E. Erten, and I. Hajnsek, "Rice Growth Monitoring by Means of X-Band Co-polar SAR: Feature Clustering and BBCH Scale," *IEEE Geoscience and Remote Sensing Letters*, vol. 12, no. 6, pp. 1218–1222, jun 2015. [Online]. Available: http://ieeexplore.ieee.org/document/7038185/

[23] G. P. Petropoulos, G. Ireland, and B. Barrett, "Surface soil moisture retrievals from remote sensing: Current status, products & future trends," *Physics and Chemistry of the Earth, Parts A/B/C*, vol. 83, pp. 36–56, 2015. [Online]. Available: http://www.sciencedirect.com/science/article/pii/S1474706515000200

[24] C. Pathe, W. Wagner, D. Sabel, M. Doubkova, and J. B. Basara, "Using ENVISAT ASAR Global Mode Data for Surface Soil Moisture Retrieval Over Oklahoma, USA," *IEEE Transactions on Geoscience and Remote Sensing*, vol. 47, no. 2, pp. 468–480, feb 2009. [Online]. Available: http://ieeexplore.ieee.org/document/4773463/

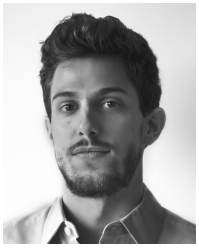

Boris Snapir received a diplome dingenieur from the Institut Suprieur de lAeronautique et de lEspace Toulouse France in 2011, and the M.Sc. and Ph.D. degrees from Cranfield University UK in 2011 and 2014, respectively. In 2015, he joined the Remote Sensing group in the School of Water, Energy and Environmental at Cranfield University, as a research fellow. His research interests include image processing, radar polarimetry, machine learning, and the application of remote sensing to Environmental monitoring.

Toby Waine received his BEng honours degree in agricultural engineering in 1995 and Engineering Doctorate (EngD) in precision agriculture in 1999, both from Cranfield University, Bedfordshire, UK. Following commercial roles as a software engineer, he returned in 2003 to Cranfield as a Research Fellow in remote sensing, working on opium poppy monitoring for the UK FCO and UNODC. Dr Waine is Lecturer in Applied Remote Sensing and Course Director for Cranfields MSc in Geographical Information Management. His current interests fall into two main themes: Land resources monitoring for crop inventory and Food security through application of remote sensing to Precision Agriculture.

Ronald Corstanje received his Ir (Engineering) degree in Environmental Science from Wageningen University in 1997 and a Ph.D in Wetland Biogeochemistry from the University of Florida in 2003. He joined the National Soil Resources Institute, Cranfield University in 2008 and is since 2017 Head of Centre, Centre for Agricultural Informatics.

Sally Redfern received a BSc honours degree in Botany from Rhodes University, Grahamstown, South Africa, in 2003. She joined Unilever R&D Colworth in the UK to work in the Life Sciences Group as a plant biochemist in 2005 and worked on various plant related projects. Since 2012 she has worked in Unilevers Refreshment Category on tea processing and agronomy research. She has a strong interest in biochemical and physiological variability within plant species. For the past three years she has been responsible for investigating the use of remote sensing tools to improve the efficiency and sustainability of primary tea processing.

Jacquie De Silva received a BSc honours degree in Life Sciences from Imperial College, London in 1981. She joined a pioneering plant molecular biology group in Unilever in the 1980s where she completed her PhD. She is a Fellow of the Royal Society of Biology and an Honorary Professor at the University of Nottingham. Her roles in Unilever have included project and science area leadership. She is interested in the application of inter-disciplinary solutions to the global challenges facing agriculture, from climate change to resource scarcity. Her research currently focuses on the use of modern breeding to improve the yield and quality of orphan crops.

Charles Kirui received the BSc in Biological sciences from Jomo Kenyatta University of Agriculture and Technology (JKUAT), Thika, Kenya. He is an Agronomist with Unilever Tea Kenya Ltd., Research and Development Department, researching on tea nutrition, harvesting, pruning, drought management and pest & diseases management. He has interest in sustainable agriculture and use of technology in tea production.

Harvest monitoring of Kenyan tea plantations with X-band SAR

Snapir, Boris

2018-02-23

Snapir B, Waine TW, Corstanje R, Redfern S, De Silva J, Kirui C, Harvest monitoring of Kenyan tea plantations with X-band SAR, IEEE Journal of Selected Topics in Applied Earth Observations and Remote Sensing, Vol. 11, Issue 3, March 2018, pp. 930-938

http://dx.doi.org/10.1109/JSTARS.2018.2799234